

Zebra-like patterns in electron cyclotron emission spectra from nonequilibrium mirror-confined laboratory plasma

M. E. Viktorov,^{1, a)} A. G. Shalashov,¹ E. D. Gospodchikov,¹ N. Yu. Semin,^{1,2} and S. V. Golubev¹

¹⁾*Institute of Applied Physics of the Russian Academy of Sciences, 46 Ulyanov str., 603950 Nizhny Novgorod, Russia*

²⁾*Lobachevsky State University, 23 Gagarina av., 603950 Nizhny Novgorod, Russia*

(Dated: 10 February 2020)

Zebra-like patterns have been observed in the electron cyclotron emission spectra from strongly nonequilibrium plasma confined in a table-top mirror magnetic trap. The analysis of the experimental data suggests that the formation of zebra-like patterns could eventually be related to modulation of the whistler waves by the magnetosonic waves excited during the abrupt ejection of electrons into a loss cone caused by the development of the whistler instability under the electron cyclotron resonance condition.

PACS numbers: 52.72.+v, 52.35.-g, 52.70.Gw

I. INTRODUCTION

The dynamics of energetic charged particles in space and laboratory magnetic traps defines the spectra of electromagnetic waves excited as a result of different types of kinetic instabilities. In some cases, the spectrum of excited waves is very wide and contains regular variations, such as frequency sweeping events. In a magnetoactive plasma a certain set of harmonics in a dynamic spectrum of plasma electromagnetic emission is often observed, which could be naturally explained as electron or ion cyclotron instability development. In space plasmas, the excitation of waves at cyclotron harmonics is observed in numerous systems, such as magnetosphere of the Earth^{1,2} and other planets³. Under laboratory conditions, the excitation of cyclotron harmonics by fast particles is observed both in linear⁴⁻⁶ and toroidal⁷ magnetic traps.

Frequently, the observation of banded harmonics in plasma electromagnetic emission is not directly related to a cyclotron instability but explained by the excitation of plasma waves under the condition of double plasma resonance which is very typical for astrophysical plasmas⁸. This phenomenon was firstly observed in the Sun radio emission^{9,10}, but also presents in the Jovian decameter radio emission^{11,12}, in the VLF hisses of the terrestrial magnetosphere¹³ and in a laboratory mirror-confined plasma¹⁴.

In all the above cases, the spectrum of plasma emission forms zebra-like patterns in a time-frequency space. Similar kind of spectral features could be also related to the variations of the medium through which the electromagnetic wave propagates. It is known that the continuous variation of plasma electron density would cause modulations to both amplitude and phase of the transmitter electromagnetic wave¹⁵. In this case the spectrum of transmitted monochromatic wave will be enriched with harmonics at the modulation frequency and the modulation strength is determined by the ratio between the plasma frequency and the incident wave frequency.

In the present paper we study the electromagnetic emission spectrum of plasma which is created and sustained by high-power microwave radiation of a gyrotron under the electron cyclotron resonance (ECR) condition in a simple mirror trap¹⁶. The detailed overview of possible types of kinetic instabilities in the present experiment is done in Ref. 17. The focus of this work is given to the study of time-frequency characteristics of plasma microwave emission at the developed discharge stage in the whistler wave frequency domain, i.e. below electron cyclotron frequency. The distinguishing feature of this kind of emission is a zebra-like dynamic spectrum with a few narrow-band stripes which are placed equidistant relative to each other. We will study the emission spectrum and discuss shortly some possible reasons of zebra-like patterns.

II. EXPERIMENTAL SETUP AND DIAGNOSTICS

The experiments were conducted with the plasma of ECR discharge sustained by gyrotron radiation (frequency 37.5 GHz, power up to 80 kW, pulse duration 1 ms) in the axially symmetric open magnetic trap¹⁷. Microwave radiation of gyrotron is launched into the discharge chamber along the trap axis. The radiation intensity in the focal plane is about 10 kW/cm² and the average power density is 100 W/cm³. We used two types of discharge chamber: (1) a cylindrical tube with inner diameter of 38 mm which is widened in the central part by the tube with inner diameter of 72 mm and of 50 mm length and (2) a straight cylindrical tube with inner diameter of 38 mm. The discharge chamber is placed in the mirror magnetic trap, produced by pulsed coils with maximum magnetic field strength of 4.3 T, the pulse duration is about 7 ms. The length of the magnetic trap is 22.5 cm for the first type of discharge chamber and for the second type discharge chamber the trap length is varied from 13 cm to 25 cm with corresponding change of the mirror ratio $R = B_{\max}/B_{\min}$. Plasma is created and supported under ECR conditions at the fundamental cyclotron harmonic corresponded to the magnetic field strength 1.34 T. The resonance surface is situated between the magnetic mirror and the center of the discharge chamber. Am-

^{a)} Author to whom correspondence should be addressed. Electronic mail: mikhail.viktorov@appl.sci-nnov.ru

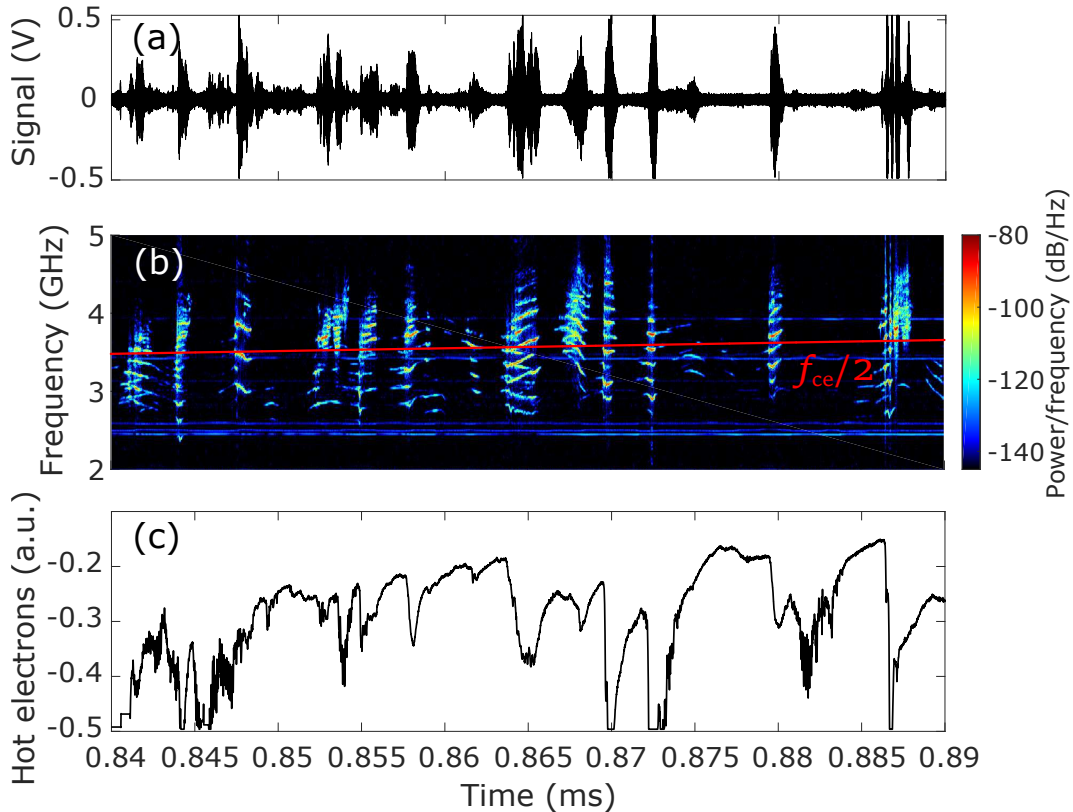


FIG. 1. (a) Waveform and (b) its dynamic spectrum of plasma microwave emission during the stationary ECR discharge, (c) the signal from the hot electron detector. The value of $f_{ce}/2$ at the trap center is shown by the red solid curve on the dynamic spectrum. The time reference starts at the moment the gyrotron is turned on, the gyrotron radiation turns off after 1 ms. The working gas is nitrogen.

bient pressure of a neutral gas (nitrogen or argon) is about 10^{-6} Torr, however it increases up to $10^{-4} - 10^{-3}$ Torr during ECR discharge.

In the experiments we study the dynamic spectrum and the intensity of enhanced electromagnetic radiation from the plasma with the use of a broadband horn antenna with a uniform bandwidth in the range from 2 to 20 GHz and the high-performance oscilloscope Keysight DSA-Z594A (analog bandwidth 59 GHz, sampling rate 160 GSamples/s). In the scope of the described experiment, the antenna bandwidth covers frequencies up to the second harmonic of electron gyrofrequency in the trap center. This method allows to analyse both the wave amplitude and its phase. The dynamic spectra is calculated from the recorded data by short-time Fourier transform windowed with Hamming window. Simultaneously, we measure precipitations of energetic electrons (10-180 keV) from the trap ends using a p-i-n diode detector with time resolution about 1 ns.

III. EXPERIMENTAL RESULTS

In the present paper we consider the developed discharge stage, which lasts from the ECR breakdown until the end of the microwave heating pulse with a duration of 1 ms. At that stage the two-component electron population is formed

containing the cold dense electrons with Maxwellian distribution ($N_c \sim 10^{13} \text{ cm}^{-3}$, $T_c \sim 300 \text{ eV}$) and less dense component of hot electrons with anisotropic distribution function ($N_h \sim 10^{11} \text{ cm}^{-3}$, mean energy $E_h \sim 10 \text{ keV}$, although energy tail is stretched up to 400 keV, see, e.g., Ref. 18).

During the developed discharge stage we registered microwave emission simultaneously in two frequency bands: (1) at frequencies about $f_{ce}/2$ and (2) at frequencies between f_{ce} and $2f_{ce}$, where f_{ce} is the electron cyclotron frequency at the trap center. Here we discuss only the first type of microwave emission, which has much higher spectral power density than the second one.

An example of the instability development is shown in Fig. 1. The recorded emission has the form of quasi-periodic bursts with a duration of about $1-5 \mu\text{s}$. The emission frequency follows $f_{ce}/2$ while the external magnetic field is slowly increasing in time. The distinctive feature of this instability is the zebra-like pattern in the dynamic spectrum of plasma emission. Note the presence of the selected frequency lines, ten or more, in the spectrum, which are arranged equidistantly with respect to each other. These frequencies are slightly evolving in time while the distance between them remains constant. Every radiation pulse is correlated with precipitations of energetic electrons from the trap ends measured with a dedicated p-i-n diode.

The detailed view of the emission spectrum for a single on-

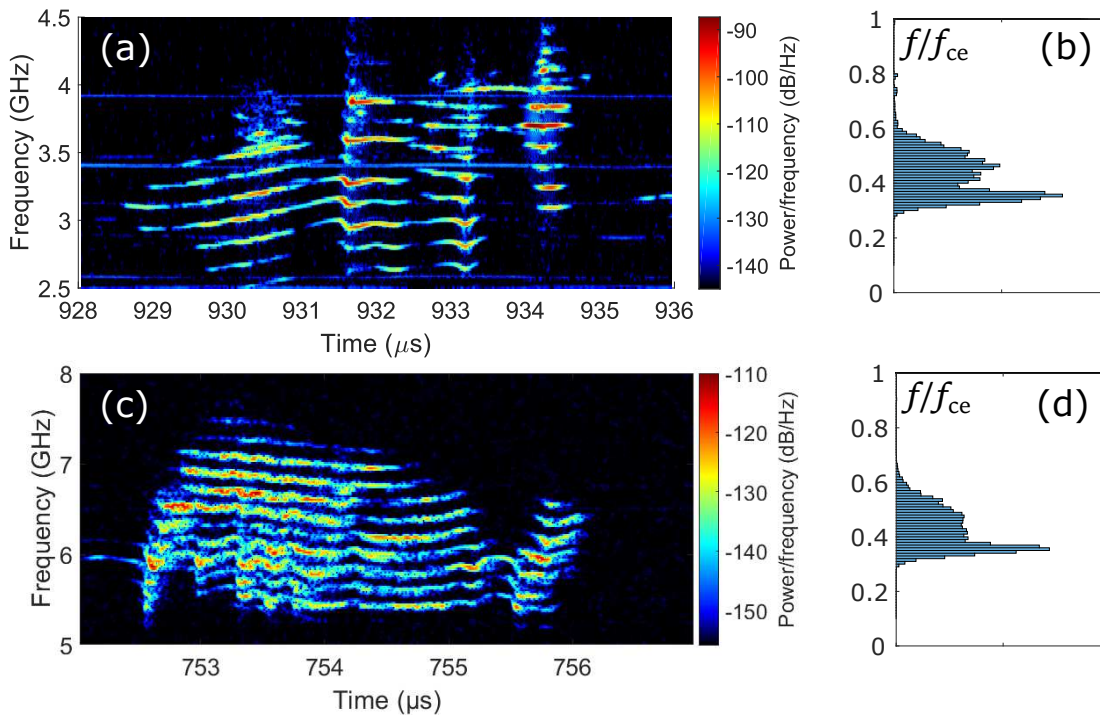


FIG. 2. An example of the dynamic spectrum of plasma microwave emission during a single event of the instability development in (a) nitrogen and (c) argon plasmas. The time reference starts at the moment the gyrotron is turned on, the gyrotron radiation turns off after 1 ms. Panels (b) and (d) show the distribution of instability events over frequency for nitrogen (b) and argon (d) discharges. Experiments were conducted with the discharge chamber type (1) – a cylindrical tube which is widened in the central part.

set of instability is shown in Fig. 2 (left panels) for discharges in nitrogen and argon. It is seen that instability development lasts about $5 \mu\text{s}$ and spectrum contains at least ten equidistantly spaced stripes for both cases.

To measure the emission bandwidth we analyzed 54 experimental shots in nitrogen plasma and 131 in argon plasma. The spectrograms were filtered using noise reduction algorithm. As a result, we obtained a set of spectrograms where only intense emissions are present. Next, all data points in a time-frequency domain were normalized over the electron cyclotron frequency in the trap center, which is evolving in time. Finally, we concatenated normalized spectrograms for a certain type of gas and retrieved a distribution of the events over frequency in the electron cyclotron frequency domain. These results are shown in Fig. 2 (right panels). For both cases, the distribution is two-humped with a more pronounced low-frequency maximum near $0.3f_{ce}$ and a wider second maximum near $0.5f_{ce}$.

Above mentioned results were obtained in a discharge chamber type (1) – a cylindrical tube which is widened in the central part, where the length of the trap and its mirror ratio are fixed. To understand the formation mechanism of the zebra-like patterns, we studied the microwave emission of plasma created in the discharge chamber in the form of a straight cylinder – type (2). We studied the instabilities during the ECR discharge in two gases (nitrogen and argon) and for a set of three different lengths of the magnetic trap L : 13.5 cm, 18.5 cm, 24 cm. With the increase of distance be-

tween the magnetic coils the mirror ratio R is also increased. The mean distance between spectral components for different experimental parameters is shown in Table I. For some regimes, we have not detected excitation of waves at frequencies below the electron gyrofrequency. This could be related to the efficiency of the ECR heating at different conditions.

TABLE I. The distance between spectral components for different experimental parameters.

L	$B_{\text{max}}/B_{\text{min}}$	N_2	Ar
13.5 cm	2	not detected	not detected
18.5 cm	3.5	$272 \pm 17 \text{ MHz}$	$322 \pm 19 \text{ MHz}$
24 cm	6	not detected	$182 \pm 12 \text{ MHz}$

IV. DISCUSSION

First of all, we note that the electromagnetic eigenmodes of the metal vacuum chamber can not be attributed to the observed spectra since this is not compatible with the equidistance of the bands in the spectrum and synchronous temporal variation of spectral lines.

The emission of dense plasma at frequencies below the electron cyclotron frequency during the ECR heating stage is most naturally related to the whistler mode instability¹⁹. At large densities of the background plasma, the cyclotron in-

stabilities of the extraordinary waves are suppressed because their dispersive properties are strongly modified by the background plasma.

Calculations of the increment of the cyclotron instability of whistler waves for the plasma parameters typical of the experiment show that the increment has the maximum near a half of the electron gyrofrequency and the peak is rather narrow²⁰. Its width under the experimental conditions is less than 100 MHz, which corresponds to the spectral width of an individual line in the frequency spectrum. Thus, the formation of a frequency comb near the fundamental frequency is most likely a result of a low frequency modulation of a medium where excited whistler waves could propagate.

For the majority of experimental shots the value of the electron cyclotron frequency in the trap center f_{ce} is in the range of 7–10 GHz. Correspondingly, the frequency of the ion cyclotron resonance is $f_{ci} \approx 0.4$ MHz for a nitrogen plasma and $f_{ci} \approx 0.1$ MHz for an argon plasma. The typical distance between spectral stripes is $\Delta f \approx 300$ MHz, see Table I. This, evidently, implies a very big ion cyclotron harmonics number $\Delta f/f_{ci} \sim 10^3$, which ensures that ion cyclotron oscillations are hardly related to the observed phenomenon.

The other low frequency process is the rotation of the plasma column due to the presence of the electric field which is transverse to the magnetic field of the trap. We estimate the frequency of $\mathbf{E} \times \mathbf{B}$ -rotation as

$$f_{rot} \approx \frac{v_{E \times B}}{a} \approx \frac{1}{2\pi f_{ce}} \frac{e\Delta\phi}{m_e a^2} \lesssim 1 \text{ MHz} < \Delta f,$$

where $v_{E \times B} = cE/B$ is the drift velocity, $E \approx \Delta\phi/a$ is the characteristic value of the radial electric field strength, $\Delta\phi \approx 100$ eV is the plasma potential drop across plasma column and $a = 1$ cm is the plasma radius.

The excitation of whistler waves leads to the falling of the resonant electrons into the loss-cone. Then the abrupt ejection of electrons from the trap ends is observed. The electron precipitation causes the formation of the ion flow from the trap which could excite ion-acoustic waves. But frequency of ion-acoustic waves is limited by the ion plasma frequency:

$$f_s \lesssim f_{pi} = \frac{1}{2\pi} \sqrt{\frac{4\pi Z^2 e^2 n_i}{m_i}} \approx (30 - 50) \text{ MHz} < \Delta f,$$

where Z is the ion charge state, $n_i = n_e/Z$ is the ion density, m_i is the ion mass (the lower f_{pi} corresponds to argon). Thus, the excitation of ion-acoustic waves could not lead to the observed frequency modulation of whistler waves.

The most appropriate option to explain the fine structure of plasma emissions is excitation of magnetosonic waves which propagates with the Alfvén velocity $v_A \sim 10^8$ cm/s. For the same perpendicular size of plasma column a we obtain

$$f_A \approx \frac{v_A}{a} = \frac{B}{a\sqrt{4\pi n_i m_i}} \approx (120 - 200) \text{ MHz} \sim \Delta f,$$

the lower value of f_A corresponds to the argon plasma. We see that this frequency fits rather well to the desired range of experimentally measured Δf .

More precise study of the zebra-like structures in whistler frequency range to support this idea is subject to our future efforts.

V. SUMMARY

The fine structure of dynamic spectra of electron cyclotron emission in whistler wave frequency range is investigated with high temporal resolution. The analysis of the experimental data suggests that formation of zebra-like patterns in the spectra could be related to the scattering of whistler waves by the low-frequency magneto-sound waves which could be excited during the abrupt ejection of electrons into the loss cone caused by the development of the electron cyclotron instability.

This research may be of interest in the context of a laboratory modeling of non-stationary processes of wave-particle interactions in space plasma, since there are a lot of open questions about the origin of some types of emissions in space cyclotron masers, especially mechanisms of fine spectral structure²¹.

ACKNOWLEDGMENTS

The work was supported by the Grants Council of the President of the Russian Federation (grant no. MK-2593.2019.2).

- ¹K. Rönmark, H. Borg, P. J. Christiansen, M. P. Gough, and D. Jones, *Space Science Reviews* **22**, 401 (1978).
- ²F. E.-L. Mazouz, J. Rauch, P. Décréau, J. Trotignon, X. Vallières, F. Darrouzet, P. Canu, and X. Suraud, *Advances in Space Research* **43**, 253 (2009).
- ³X. Tao, R. M. Thorne, R. B. Horne, S. Grimald, C. S. Arridge, G. B. Hospodarsky, D. A. Gurnett, A. J. Coates, and F. J. Cray, *Journal of Geophysical Research: Space Physics* **115**, A12204 (2010).
- ⁴R. Ikezoe, M. Ichimura, T. Okada, M. Hirata, T. Yokoyama, Y. Iwamoto, S. Sumida, S. Jang, K. Takeyama, M. Yoshikawa, J. Kohagura, Y. Shima, and X. Wang, *Physics of Plasmas* **22**, 090701 (2015).
- ⁵B. Van Compernelle, X. An, J. Bortnik, R. M. Thorne, P. Pribyl, and W. Gekelman, *Phys. Rev. Lett.* **114**, 245002 (2015).
- ⁶B. V. Compernelle, X. An, J. Bortnik, R. M. Thorne, P. Pribyl, and W. Gekelman, *Plasma Physics and Controlled Fusion* **59**, 014016 (2016).
- ⁷S. Sharapov, B. Alper, H. Berk, D. Borba, B. Breizman, C. Challis, I. Classen, E. Edlund, J. Eriksson, A. Fasoli, E. Fredrickson, G. Fu, M. Garcia-Munoz, T. Gassner, K. Ghantous, V. Goloborodko, N. Gorelenkov, M. Gryaznevich, S. Hacquin, W. Heidbrink, C. Hellesen, V. Kiptily, G. Kramer, P. Lauber, M. Lilley, M. Lisak, F. Nabais, R. Nazikian, R. Nyqvist, M. Osakabe, C. P. von Thun, S. Pinches, M. Podesta, M. Porkolab, K. Shinohara, K. Schoepf, Y. Todo, K. Toi, M. V. Zeeland, I. Voitsekovich, R. White, V. Yavorskij, I. E. TG, and J.-E. Contributors, *Nuclear Fusion* **53**, 104022 (2013).
- ⁸V. V. Zheleznyakov, E. Y. Zlotnik, V. V. Zaitsev, and V. E. Shaposhnikov, *Usp. Fiz. Nauk* **186**, 1090 (2016).
- ⁹V. V. Zheleznyakov and E. Y. Zlotnik, *Solar Physics* **43**, 431 (1975).
- ¹⁰V. V. Zheleznyakov and E. Y. Zlotnik, *Solar Physics* **44**, 461 (1975).
- ¹¹W. S. Kurth, G. B. Hospodarsky, D. A. Gurnett, A. Lecacheux, P. Zarka, M. D. Desch, M. L. Kaiser, and W. M. Farrell (2001).
- ¹²G. Litvinenko, V. Shaposhnikov, A. Konovalenko, V. Zakharenko, M. Panchenko, V. Dorovsky, A. Brazhenko, H. Rucker, V. Vinogradov, and V. Melnik, *Icarus* **272**, 80 (2016).
- ¹³E. E. Titova, A. G. Demekhov, D. L. Pasmanik, V. Y. Trakhtengerts, J. Manninen, T. Turunen, and M. J. Rycroft, *Geophysical Research Letters* **34**, L02112 (2007).

- ¹⁴D. Mansfeld, M. Viktorov, S. Golubev, and V. Zaitsev, *Planetary and Space Science* **164**, 158 (2018).
- ¹⁵M. Yang, X. Li, K. Xie, and Y. Liu, *Physics of Plasmas* **22**, 022120 (2015).
- ¹⁶M. Viktorov, D. Mansfeld, and S. Golubev, *EPL (Europhysics Letters)* **109**, 65002 (2015).
- ¹⁷A. G. Shalashov, M. E. Viktorov, D. A. Mansfeld, and S. V. Golubev, *Physics of Plasmas* **24**, 032111 (2017).
- ¹⁸S. V. Golubev, I. V. Izotov, D. A. Mansfeld, and V. E. Semenov, *Review of Scientific Instruments* **83**, 02B504 (2012).
- ¹⁹A. V. Vodopyanov, S. V. Golubev, A. G. Demekhov, V. G. Zorin, D. A. Mansfeld, S. V. Razin, and V. Y. Trakhtengerts, *Plasma Physics Reports* **31**, 927 (2005).
- ²⁰A. G. Demekhov and V. Y. Trakhtengerts, *Radiophysics and Quantum Electronics* **29**, 848 (1986).
- ²¹R. A. Treumann, *The Astronomy and Astrophysics Review* **13**, 229 (2006).